Structure Determination of Homoleptic Au^I, Ag^I, and Cu^I Aryl/Alkylethynyl Coordination Polymers by X-ray Powder Diffraction

Stephen S. Y. Chui, Miro F. Y. Ng, and Chi-Ming Che*[a]

Abstract: This article describes the structure determination of five homoleptic d^{10} metal–aryl/alkylacetylides [RC≡CM] (M = Cu, R = *t*Bu **1**, *n*Pr **2**, Ph **3**; R = Ph, M = Ag **4**; Au **5**) by using X-ray single-crystal and powder diffraction. Complex **1**·C_6H_6 reveals an unusual Cu_{20} catenane cluster structure that has various types of *t*BuC≡C→Cu coordination modes. By using this single-crystal structure as a starting model for subsequent Rietveld refinement of X-ray powder diffraction data, the structure of the powder synthesized from CuI and *t*BuC≡CH was found to have the same structure as **1**. Complex **2** has an extended sheet structure consisting of discrete zig-zag Cu_4 subunits connected through bridging *n*PrC≡C groups. Complex **3** forms an infinite chain structure with extended Cu–Cu ladders (Cu–Cu = 2.49(4)–2.83(2) Å). The silver(I) congener **4** is iso-structural to **3** (average Ag–Ag distance 3.11 Å), whereas the gold(I) analogue **5** forms a Au···Au honeycomb network with PhC≡C pillars (Au–Au = 2.98(1)–3.26(1) Å). Solid-state properties including photoluminescence, ν(C≡C) stretching frequencies and thermal stability of these polymeric systems are discussed in the context of the determined structures.

Keywords: alkyne ligands · chain structures · layered compounds · structure elucidation · X-ray diffraction

Introduction

Electron rich d^{10} metal acetylide complexes have been receiving considerable attention due to their rich structural diversity,[1] intriguing photoluminescent properties,[2] as well as potential applications in organic optoelectronics[3] and luminescence signalling.[4] Homoleptic [RC≡CM] complexes constitute a useful class of metal–acetylide precursor materials for the syntheses of related organometallic complexes.[5] To our knowledge, well-characterized homoleptic [RC≡CM] compounds are sparse in literature. In 1993, Weiss and co-workers reported a [(*t*BuC≡CCu)$_{24}$] cluster.[6] Later the gold(I) double-catenane complex [{(*t*BuC≡CAu)$_6$}$_2$] was reported by Mingos and co-workers.[7] Recently Mingos' group also prepared an unprecedented rhombohedral silver(I) cluster cage [(*t*BuC≡C)$_{12}$Au$_{14}$X]Y by using various anionic templates (X = Cl, Br; Y = OH, BF_4).[8] All these examples display diverse coordination modes and there are extensive intermolecular interactions between [RC≡CM] units. Apparently, the [(RC≡CM)$_n$] aggregates have a poor solubility unless the R group is sterically encumbered. Many [(RC≡CM)$_n$] compounds are therefore believed to have polymeric structures, though these structures are poorly understood.

Past and recent developments in structure determinations using X-ray powder diffraction data have become increasingly important for intractable crystalline materials. Early contributions in this field by Zachariasen and Ellinger,[9] Kokotailo and Breck,[10] and Werner and Berg[11] had been witnessed to tackle some of the difficult structural problems. With the advances in radiation source, detector technology, and computing algorithms, a wide range of unknown structures of organic, inorganic, organometallic, and protein systems have been determined by using powder diffraction data.[12]

To acquire insights on the structures of polymeric [(RC≡CM)$_n$] solids, a program on structure determination from X-ray powder diffraction data was initiated. Preliminary experiments revealed that this class of [(RC≡CM)$_n$] compounds could be polycrystalline with moderate X-ray diffracting strength. Elemental analyses confirmed the phase purity of the [(RC≡CM)$_n$] solids in accordance with their formulations.[13] Herein we describe the structure determination of five unprecedented solid-state structures of [(RC≡CM)$_n$] solids (R = *t*Bu, M = Cu **1**; R = *n*Pr, M = Cu **2**; R = Ph,

[a] Dr. S. S. Y. Chui, M. F. Y. Ng, Prof. C.-M. Che
Department of Chemistry
HKU-CAS Joint Laboratory of New Materials and
Open Laboratory of Chemical Biology of The Institute of
Molecular Technology for Drug Discovery and Synthesis
Chong Yuet Ming Building, The University of Hong Kong
Pokfulam, Hong Kong (China)
Fax: (+852) 291-55-176
E-mail: cmche@hku.hk

Supporting information for this article is available on the WWW under http://www.chemeurj.org/ or from the author.

 DOI: 10.1002/chem.200400881 © 2005 Wiley-VCH Verlag GmbH & Co. KGaA, Weinheim

M = Cu **3**; R = Ph, M = Ag **4**; and R = Ph, M = Au **5**) using laboratory X-ray powder diffraction data. We found that **1** possesses a Cu_{20} cluster structure, while **2–5** have either one- or two-dimensional polymeric structures. Their solid-state properties such as photoluminescence, thermal stability and ν(C≡C) stretching frequencies have been recorded and are discussed in connection to their structures.

Experimental Section

All starting materials were used as received without further purification. Samples **1–5** were prepared according to published methods.[13] Single crystals of **1** (ca. 5%) were obtained by slow diffusion of 1:1 (v/v) ethanol/acetone mixture into benzene solution (2 mL) over one month. Attempts to obtain crystals of **2–5** with sizes suitable for structure determination were not successful, since the as-precipitated products were insoluble in common organic solvents. Elemental analyses were performed at the Institute of Chemistry, Chinese Academy of Science in Beijing. Elemental analysis calcd (%) for **1**: C 49.82, H 6.23; found: C 49.46, H 6.29; elemental analysis calcd (%) for **2**: C 45.97, H 5.36; found: C 45.65, H 5.33; elemental analysis calcd (%) for **3**: C 58.35, H 3.03; found: C 58.30, H 3.01; elemental analysis calcd (%) for **4**: C 45.97, H 2.39; found: C 45.75, H 2.20; elemental analysis calcd (%) for **5**: C 32.24, H 1.68; found: C 32.10, H 1.58.

Solid-state photoexcitation and emission spectra were recorded on Spex Fluorolog Model I168 fluorescence spectrophotometer equipped with Hamamatsu R-928 photomultiplier tube. Low-temperature (77 K) spectra were recorded by immersing a quartz sample tube in a quartz Dewar flask filled with liquid N_2. FT-IR spectra (KBr) were collected on a Bio-Rad FTS-7 Fourier transform infrared spectrophotometer (4000–400 cm^{-1}). Thermal gravimetric curves were recorded under nitrogen atmosphere using Perkin Elmer TGA7 Analyzer.

Intensity data of a capillary-sealed single crystal of **1** with size $0.5\times0.4\times0.05$ mm^3 was collected at 233 K on a Bruker Smart Apex CCD diffractometer with graphite-monochromated $Mo_{K\alpha}$ ($\lambda = 0.71073$ Å) radiation. Data reduction and absorption correction of the data were applied by using the SAINT and SADABS routines,[14a] respectively. Structure solution (SHELXS)[14b] was obtained by direct methods and the structure refinement (SHELXL) was performed by full-matrix least-squares methods on $|F^2|$ algorithm in SHELX-97 suite X-ray programs (version 6.10).[14c]

All samples **1–5** were freshly prepared, dried, and ground into a fine powder. Step-scanned X-ray powder diffraction data were collected on Philips PW3710 powder diffractometer by using graphite-monochromated $Cu_{K\alpha}$ ($\lambda = 1.5406$ Å, Ni-filter) radiation, operated at 40 kV and 30 mA. Data collection for **4** and **5** were carried out in the dark environment. Samples were unpacked and reloaded onto the sample holders for replication data collections to minimize the systematic errors from particle statistics and preferred orientation of the samples. All samples were free of known oxides and metal impurities checked by ICCD database match search. Data collection parameters of 2–60° (2θ), step size = 0.02°, and scan speed = 0.004° s^{-1} were used to optimize the count statistics and peak shape profiles. Unit-cell determination from DICVOL91[15] program was achieved by indexing the first 20 peak positions in each diffraction pattern. Intensity extraction was performed by Pawley fit method[16] and the calculated intensities for those *hkl* reflections were used to evaluate the systematic absences for the lattice type and space group. Initial structural models were built according to standard bond lengths and angles.[17] These models were used to calculate a large number of trial structure solutions using simulated annealing algorithm implemented in DASH.[18a] A chemically sensible solution was selected and subjected to the Rietveld profile refinement[18b] by using the GSAS program.[18c] Details of structure determination from powder diffraction data and Rietveld refinement plots of **1–5** are summarized in the Supporting Information. Crystallographic data for polymers **2–5** are given in Table 1. Molecular graphics

Table 1. Structure determination and refinement results of **1–5** from powder data.

	1	**2**	**3**	**4**	**5**
crystal system	triclinic	monoclinic	monoclinic	monoclinic	triclinic
space group	$P\bar{1}$	$P2_1/n$	$P2_1$	$P2_1$	$P\bar{1}$
a [Å]	15.982(5)	19.253(4)	15.451(3)	18.512(4)	6.238(1)
b [Å]	16.099(5)	4.221(1)	5.287(2)	4.971(1)	7.531(1)
c [Å]	26.909(9)	14.767(3)	10.283(2)	13.413(3)	15.017(1)
α [°]	79.77(2)	90.00(0)	90.00(0)	90.00(0)	86.90(1)
β [°]	79.48(5)	117.56(2)	109.23(1)	111.68(1)	78.73(1)
γ [°]	81.72(4)	90.00(0)	90.00(0)	90.00(0)	83.26(1)
V [Å^3]	5821.5(4)	1063.8(4)	793.3(5)	1146.9(6)	686.8(2)
M_r	5787.1	1045.2	658.0	835.9	1192.4
ρ_{calcd} [g cm^{-1}]	1.506	1.632	1.379	1.210	2.883
2θ range [°]	2–35	2–60	3–60	2–55	2–60
figure of merit[a]	$M(20) = 10.8$	$M(18) = 36.8$	$M(20) = 24.9$	$M(20) = 21.0$	$M(20) = 10.3$
(DICVOL91indexed cell)[b]	$F(20) = 41.7$ (0.0137, 35)	$F(18) = 28.8$ (0.006, 46)	$F(20) = 38.5$ (0.0113, 46)	$F(20) = 48.8$ (0.0137, 30)	$F(20) = 20.4$ (0.0175, 56)
reflections	1488	581	563	624	759
observed reflections	1649	2899	2850	2650	2899
variables	12	83	131	132	134
restraints	10	29	30	37	38
R_p [%][c]	5.27	5.19	6.60	11.28	9.08
R_{wp} [%][d]	7.68	7.55	9.08	15.27	12.95
R_{wp}(expected) [%][e]	3.23	3.70	5.51	6.88	7.37
goodness of fit	2.39	2.06	1.67	2.54	1.84
max. [shift/esd]^2 (mean)	0.28 (0.06)	1.05 (0.15)	0.66 (0.07)	2.41 (0.28)	1.44 (0.20)

[a] Figure of merit $M(20)$ and $F(20)$ were described in P. M. De Wolff, *J. Appl. Crystallogr.* **1968**, *1*, 108–113. [b] Initial unit cell parameters are empirically determined by indexing peak positions of diffraction patterns using DICVOL91 program and these are subsequently refined by Rietveld method in GSAS program to give the values listed. [c] $R_p = \Sigma_i |y_{i,o} - y_{i,c}| / \Sigma_i |y_{i,o}|$. [d] $R_{wp} = [\Sigma_i w_i (y_{i,o} - y_{i,c})^2 / \Sigma_i w_i (y_{i,o})^2]^{1/2}$. [e] Expected $R_{wp} = R_{wp}/\chi^2$; $\chi^2 = \Sigma_i w_i (y_{i,o} - y_{i,c})^2 / (N_{obs} - N_{var})$ in which $y_{i,o}$ and $y_{i,c}$ are the observed and calculated intensities at point i of the profile, respectively. N_{obs} is the number of theoretical Bragg peaks in the 2θ range considered. N_{var} is number of the refined parameters. Statistical weights w_i are normally taken as $1/y_{i,o}$.

© 2005 Wiley-VCH Verlag GmbH & Co. KGaA, Weinheim

were created by the crystal structure visualization program Mercury version 1.2 that was downloaded free of charge.[19] CCDC-242487 (single crystal data for **1**) and CCDC-242488–242492 (powder diffraction data for **1**–**5**, respectively) contain the supplementary crystallographic data for this paper. These data can be obtained free of charge from The Cambridge Crystallographic Data Centre via www.ccdc.cam.ac.uk/data_request/cif.

Results and Discussion

Structure descriptions of 1–5: Crystal structures of **1** and its benzene solvate were obtained by X-ray powder and single-crystal diffraction data,[20] respectively. Figure 1 depicts the ORTEP diagram of the molecular structure of **1**, showing the Cu_{20} cluster with twenty crystallographically independent *t*BuC≡CCu units. The molecular symmetry has no inversion center, but a pseudo C_2 axis passes through the midpoints of Cu10–Cu16, Cu9–Cu15, and Cu14–Cu20 bonds. The cluster architecture can be viewed as an interlocking of a distorted Cu_8 ring with two puckered hexagonal Cu_6 rings (see Figure 2), supported by various *t*BuC≡C→Cu coordination modes. The bond lengths are given in Table 2. The Cu–C distances are 1.862(6)–2.471(7) Å. Altogether there are two $\mu,\eta^{1,1}$-C≡C→Cu_2, and eight $\mu,\eta^{1,2}$-C≡C→Cu_2 bridging modes are associated with the copper atoms in the Cu_8 and Cu_6 rings. In addition, four $\mu_3,\eta^{1,1,2}$-C≡C→Cu_3 and six $\mu_4,\eta^{1,1,1,2}$-C≡C→Cu_4 bridging modes are found to fuse the Cu atoms of different rings together. Extensive Cu–Cu contacts of 2.498–3.482(1) Å are found and similar Cu···Cu contacts were also observed in various types of copper(I) sulfido/selenido/tellurido phosphine nanoclusters.[21] Some of these Cu–Cu distances are less than the sum of metallic radii (2.56 Å) and the van der Waals radii (2.8 Å)[22a] of two Cu atoms, revealing the occurrence of cuprophilic interaction.[23]

The isolation of **1** not only represents a rare example of a homoleptic Cu_{20} cluster with an unprecedented copper(I) ring catenation, but also provides a starting model for structural elucidation of the fine powder obtained from rapid precipitation. The structure refinement for the observed diffraction data of the fine powder using this Cu_{20} model afforded a good agreement ($R_p = 5.27\%$, $R_{wp} = 7.68\%$) between the experimental and calculated data. The crystal structure derived from X-ray powder diffraction data is a nearly identical cluster structure to the one determined by single-crystal X-ray analysis and the observed Cu–C and Cu–Cu distances are 1.822–2.640(5) Å and 2.403–3.457(1) Å, respectively. It is noted that the unit cell volume decreases from 6552 Å^3 for $[(t\text{BuC}{\equiv}\text{CCu})_{20}]\cdot C_6H_6$ (determined by single-crystal data) to 5821 Å^3 for $[(t\text{BuC}{\equiv}\text{CCu})_{20}]$ (determined by indexed powder diffraction data), implying removal of benzene solvent molecules from the crystal lattice leads to closer molecular packing of the Cu_{20} clusters.

Figure 3 (top) depicts the polymeric sheet structure of **2**. It consists of two crystallographic non-equivalent Cu atoms Cu1 and Cu2 and two bridging *n*PrC≡C groups. A discrete zig-zag Cu_4 subunit is formed by connecting Cu1 and its inversion-symmetry equivalence Cu1A. As shown in Table 3, the observed Cu1–Cu2 and Cu1–Cu1A distances are 2.61(2) and 2.44(3) Å respectively. Two distinctive coordination modes, $\mu,\eta^{1,2}$-C≡C→Cu_2 and $\mu_3,\eta^{1,1,2}$-C≡C→Cu_3 are found with Cu–C distances of 1.96(1)–2.23(1) Å. As viewed from the [101] direction, each Cu_4 subunit is interconnected to the four neighboring subunits through the acetylenic carbons C10 of the $\mu,\eta^{1,2}$-C≡CPr ligands to generate an extended two-dimensional sheet structure. Within the subunit a $\mu_3,\eta^{1,1,2}$-bridging coordination to Cu1, Cu1A and Cu2 is found. This type of metal–ligand connectivity renders the propyl groups pillaring perpendicular to the plane of the sheet (Figure 3, bottom). The average intermolecular aliphatic C–H···H–C separation of 2.03 Å indicates significant hydrophobic interaction throughout these propyl chains.

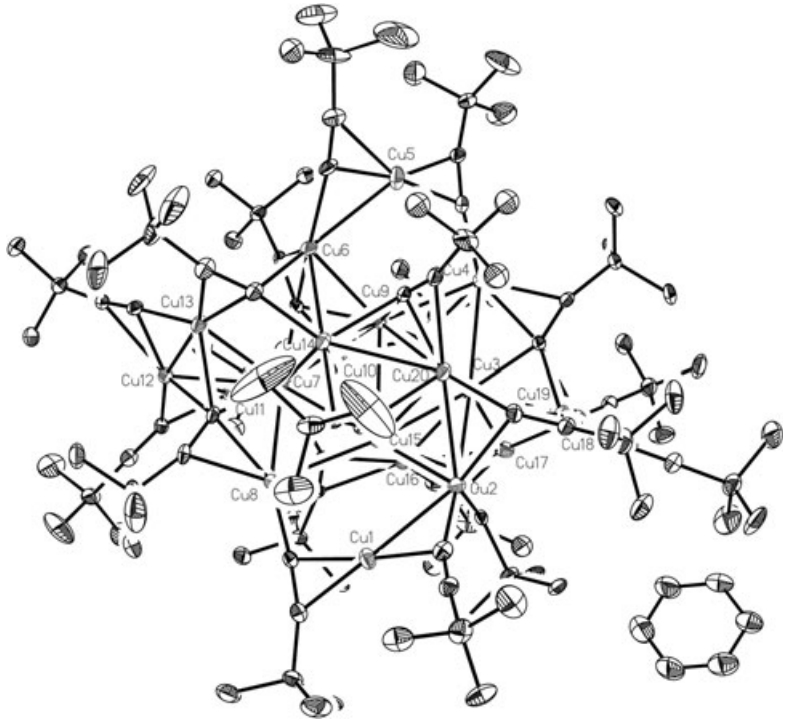

Figure 1. 35% ORTEP diagram of crystal structure of Cu_{20} molecular cluster **1**. All hydrogen atoms are omitted for clarity. The Cu···Cu contacts are 2.498–3.482(1) Å. The Cu···C and C···C distances are 1.862–2.471(6) Å and 1.165–1.244(8) Å, respectively.

 © 2005 Wiley-VCH Verlag GmbH & Co. KGaA, Weinheim

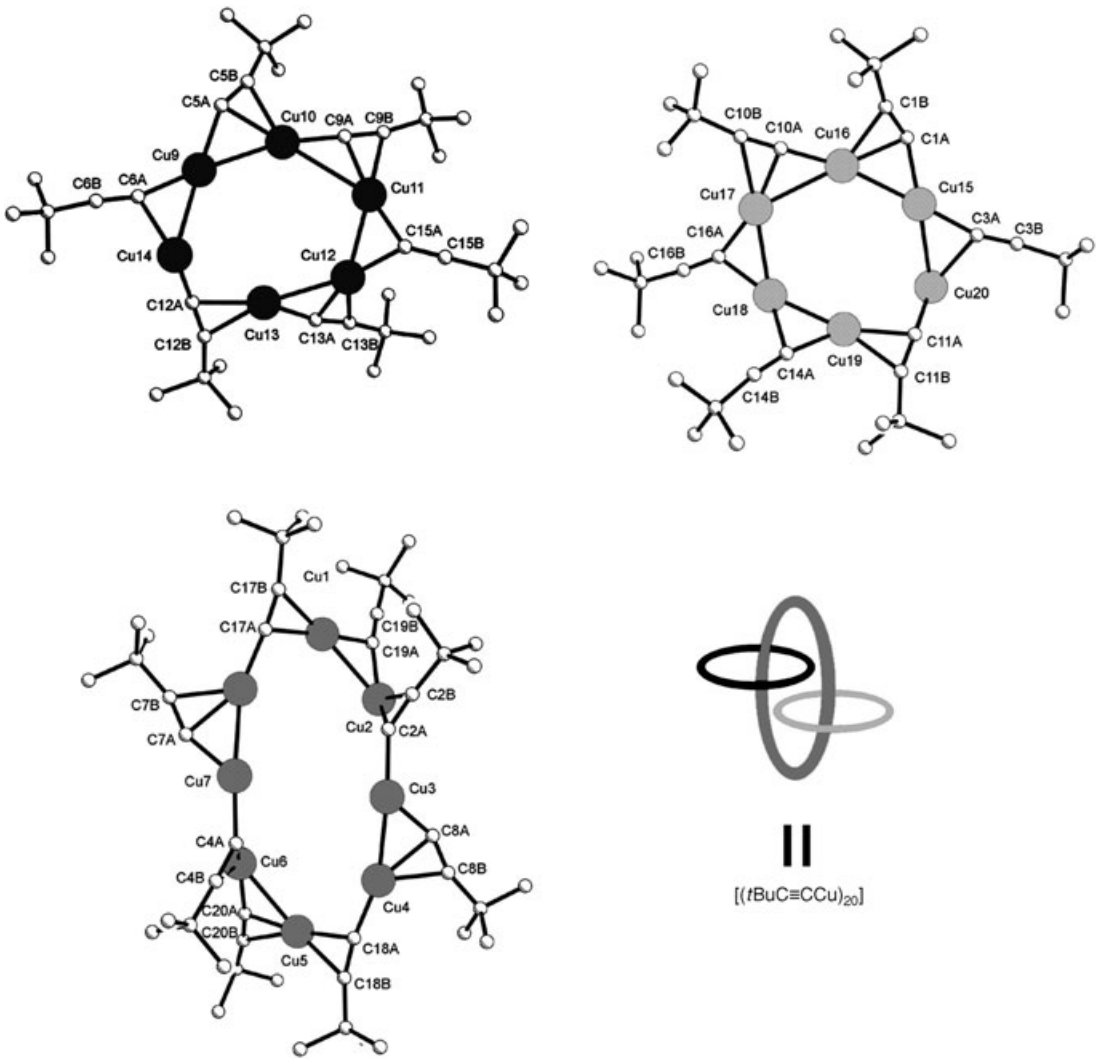

Figure 2. Schematic drawing showing the cluster assembly of three interlocking [*t*BuC≡CCu] rings: Central Cu_8 unit (medium gray) and two peripheral Cu_6 units (dark gray and light gray).

Changing the R group from an alkyl to an aryl moiety produces a [{PhC≡CCu}$_\infty$] chain polymer **3**. As shown in Figure 4 (top), a crystallographic 2_1 screw axis is parallel to the polymer chain direction which bisects Cu–Cu bonds such that the PhC≡C groups alternatively project up and down along the chain. Both Cu1 and Cu2 atoms adopt the same $\mu,\eta^{1,2}$-C≡C bridging mode and the refined Cu–Cu distances are 2.49(4)–2.83(2) Å, while the Cu–C distances are 1.95(1)–2.63(1) Å (Table 3). The longer Cu–C distances such as Cu1–C17 and Cu2–C7 are simply regarded as kinds of weak Cu···C bonding interaction because they lie between the sum of covalent radii (2.2 Å) and van der Waals radii (3.1 Å) for a pair of Cu and C atoms. For Cu–Cu contacts less than the sum of van der Waals radii for two Cu^I ions, the presence of closed-shell cuprophilic interaction along the chain is evident. The occurrence of this ladderlike chain topology is unprecedented and different from the discrete Cu_4 zig-zag subunits reported in previous examples [$(PhC{\equiv}CCu)_4(Ph_2PCH_2(CH_2OCH_2)_2CH_2PPh_2)_2$],[5i] [{PhC≡CCu$(PMe_3)$}$_4$],[38] and **2**. Figure 4 (bottom) depicts the packing diagrams of the polymer chains viewed along [010] direction, showing extensive long-range intermolecular interactions among the aromatic rings throughout the crystal lattice. Very weak C–H···π interaction ($d > 3.35$ Å) and insignificant π···π stacks ($d > 3.7$ Å) are noted.

For the powder diffraction pattern of **4** (Figure S4 in the Supporting Information), the first three diffraction peak maxima (5.19°, 7.12° and 10.27°) are apparently shifted toward the low 2θ angle, relative to those (6.08°, 9.16° and 12.12°) in the pattern of **3** (Figure S3 in the Supporting Information). The origin of this angular shift in **4** is not known. In addition, these three strong peaks have similar relative intensity variation in both cases. Indexing the peak positions of the XRD pattern of **4** gave similar monoclinic cell parameters to those found in **3**, but the associated unit cell volume is larger (Table 1) indicating that **4** might structurally resemble the [(PhC≡CCu)$_\infty$] polymer. The slightly expanded metal–ligand connectivity for the Ag and PhC≡C

© 2005 Wiley-VCH Verlag GmbH & Co. KGaA, Weinheim

Table 2. Selected bond lengths [Å] of **1** from single-crystal structure solution.[a]

Cu–Cu contacts within the Cu_8 ring unit							
Cu1–Cu2	2.614(1)	Cu2–Cu3	3.482(1)	Cu3–Cu4	2.609(1)	Cu4–Cu5	3.209(1)
Cu5–Cu6	2.718(1)	Cu6–Cu7	3.456(1)	Cu7–Cu8	2.609(1)	Cu8–Cu1	3.166(1)
Cu–Cu contacts within the two Cu_6 ring units							
Cu9–Cu10	2.590(1)	Cu10–Cu11	2.992(1)	Cu11–Cu12	2.498(1)		
Cu12–Cu13	2.580(1)	Cu13–Cu14	3.172(1)	Cu9–Cu14	2.755(1)		
Cu15–Cu16	2.557(1)	Cu16–Cu17	2.838(1)	Cu17–Cu18*	2.783(1)		
Cu18*–Cu19	2.733(1)	Cu19–Cu20	3.125(1)	Cu15–Cu20	2.713(1)		
Cu–Cu contacts between the Cu_6-Cu_8 ring units							
Cu2–Cu15	2.583(1)	Cu2–Cu20	2.577(1)	Cu3–Cu9	2.703(1)	Cu3–Cu15	2.735(1)
Cu3–Cu16	2.665(1)	Cu3–Cu17	3.043(1)	Cu3–Cu18*	2.792(2)	Cu3–Cu19	2.700(1)
Cu3–Cu20	2.916(1)	Cu4–Cu9	2.618(1)	Cu6–Cu14	2.591(1)	Cu6–Cu9	2.585(1)
Cu7–Cu9	2.749(1)	Cu7–Cu10	2.637(1)	Cu7–Cu12	2.918(1)	Cu7–Cu13	2.674(1)
Cu7–Cu14	2.930(1)	Cu7–Cu15	2.759(1)	Cu8–Cu15	2.659(1)	Cu9–Cu15	2.841(1)
Cu9–Cu20	3.018(1)	Cu14–Cu15	3.038(1)	Cu14–Cu20	2.712(1)		
C≡C bond lengths							
C1A–C1B	1.253(7)	C6A–C6B	1.224(8)	C11A–C11B	1.236(7)	C16A–C16B	1.212(8)
C2A–C2B	1.224(7)	C7A–C7B	1.224(8)	C12A–C12B	1.229(8)	C17A–C17B	1.235(8)
C3A–C3B	1.217(7)	C8A–C8B	1.234(7)	C13A–C13B	1.211(8)	C18A–C18B	1.234(8)
C4A–C4B	1.244(7)	C9A–C9B	1.220(8)	C14A–C14B	1.165(8)	C19A–C19B	1.198(8)
C5A–C5B	1.221(8)	C10A–C10B	1.227(8)	C15A–C15B	1.223(8)	C20A–C20B	1.185(8)
Cu–C bond lengths							
$\mu,\eta^{1,1}$-(C≡C)→Cu_2 mode		$\mu,\eta^{1,2}$-(C≡C)→Cu_2 mode					
C15A–Cu11	1.909(8)	C9A–Cu10	1.906(6)	C10A–Cu17	1.963(6)	C13A–Cu12	2.003(6)
C15A–Cu12	1.936(6)	C9B–Cu11	2.166(7)	C10B–Cu17	2.254(7)	C13B–Cu12	2.306(6)
C19A–Cu1	1.949(6)	C9A–Cu11	1.988(6)	C10A–Cu16	1.893(6)	C13A–Cu13	1.925(7)
C19A–Cu2	1.952(7)	C14A–Cu18*	2.015(7)	C16A–Cu18*	1.862(6)	C17A–Cu1	2.002(5)
		C14B–Cu18*	2.163(7)	C16B–Cu18*	2.330(7)	C17B–Cu1	2.136(7)
		C14A–Cu19	1.968(6)	C16A–Cu17	1.900(7)	C17A–Cu8	1.899(6)
		C18A–Cu5	1.999(5)	C20A–Cu5	1.953(8)		
		C18B–Cu5	2.138(6)	C20B–Cu5	2.471(7)		
		C18A–Cu4	1.903(6)	C20A–Cu6	1.948(6)		
$\mu_3,\eta^{1,1,2}$-(C≡C)→Cu_3 mode							
C3A–Cu14	2.086(5)	C6A–Cu20	2.076(6)	C11A–Cu19	2.092(6)	C12A–Cu13	2.096(6)
C3B–Cu14	2.182(6)	C6B–Cu20	2.168(6)	C11B–Cu19	2.122(6)	C12B–Cu13	2.107(6)
C3A–Cu15	1.942(6)	C6A–Cu9	1.944(6)	C11A–Cu2	2.176(6)	C12A–Cu6	2.225(7)
C3A–Cu20	2.224(5)	C6A–Cu14	2.232(6)	C11A–Cu20	1.916(6)	C12A–Cu14	1.920(6)
$\mu_4,\eta^{1,1,1,2}$-(C≡C)→Cu_4 mode							
C1A–Cu16	2.113(5)	C2A–Cu2	2.231(6)	C4A–Cu6	2.192(6)	C5A–Cu10	2.096(5)
C1B–Cu16	2.157(6)	C2B–Cu2	2.228(6)	C4B–Cu6	2.179(6)	C5B–Cu10	2.126(6)
C1A Cu7	2.063(6)	C2A–Cu15	2.159(6)	C4A–Cu7	1.968(6)	C5A–Cu9	2.008(6)
C1A–Cu8	2.282(5)	C2A–Cu16	2.202(6)	C4A–Cu9	2.142(5)	C5A–Cu3	2.103(6)
C1A–Cu15	2.008(6)	C2A–Cu3	1.973(6)	C4A–Cu10	2.207(6)	C5A–Cu4	2.228(5)
C7A–Cu8	2.078(6)	C8A–Cu4	2.074(5)				
C7B–Cu8	2.109(5)	C8B–Cu4	2.119(5)				
C7A–Cu12	2.373(6)	C8A–Cu3	2.005(5)				
C7A–Cu13	2.124(6)	C8A–Cu18*	2.283(5)				
C7A–Cu7	1.991(6)	C8A–Cu19	2.144(6)				

[a] * represents the mean position of the two disordered components: Cu18 and Cu18′.

entities is not unexpected, because Ag–Ag (3.11–3.15(1) Å) and Ag–C bond lengths (2.12–2.32(2) Å) are in general slightly longer than Cu–Cu and Cu–C bonds.[17] Attempts to locate a chemically sensible trial structure using the observed XRD data were unsuccessful. Thus a model of $[(PhC{\equiv}CAg)_\infty]$ derived from that of $[(PhC{\equiv}CCu)_\infty]$ was readjusted and used to refine the diffraction data of **4**. With the use of Ag–C distances restraints, the structure refinement finally attained a stable convergence and the overall polymeric structure of **4** is shown in Figure 5 (top). Unlike **3**, the degree of zig-zag folding of the ladderlike Ag–Ag chain is greater than that for the Cu–Cu chain as they have different M-M-M angles (105.2° for Ag and 163.5° for Cu). The refined Ag–Ag distances are approximately 3.13(1) Å, which fall between the metallic radius (2.89 Å)[22b] and the sum of van der Waals radii of two silver atoms (3.4 Å).[22b] This could be taken as evidence to reflect that no or only very weak Ag^I–Ag^I interactions are present[24] in the chain. In addition, the interchain packing diagram (Figure 5, bottom) reveals similar packing of phenyl groups as shown

 © 2005 Wiley-VCH Verlag GmbH & Co. KGaA, Weinheim

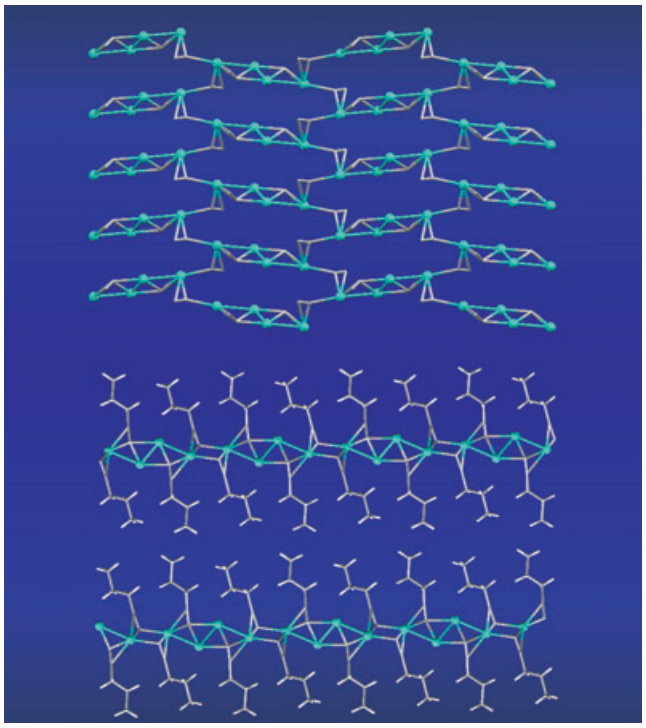

Figure 3. Top: Layered structure of **2** showing $\mu,\eta^{1,2}$- and $\mu_3,\eta^{1,1,2}$-coordination modes among the zig-zag Cu_4 and *n*PrC≡C entities. Only acetylenic carbon and copper atoms are shown. Bottom: Side view of the *n*PrC≡C-pillared layered structure.

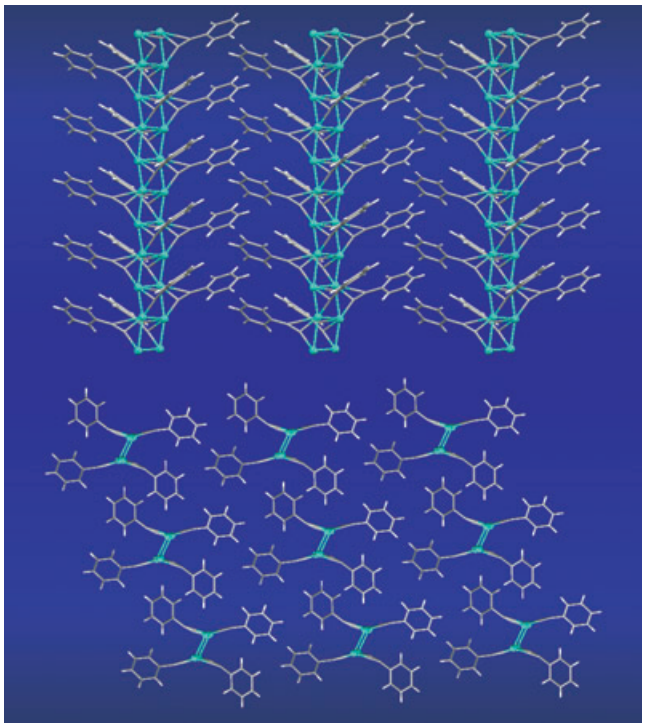

Figure 4. Top: Polymeric chain **3** showing $\mu,\eta^{1,2}$-bridging ligands PhC≡C connected to Cu^{I} ions. Bottom: Perspective view of solid-state packing of chains **3** in [010] direction.

in **3**. The shortest intermolecular aromatic C–H···H–C distance is 3.3 Å, which induces apparent organic–inorganic segregation for the phenyl rings stacking and Ag–Ag double-chain.

The structure determination was further continued for the gold congener $[(PhC{\equiv}CAu)_\infty]$ (**5**). A lower crystal symmetry of triclinic $P\bar{1}$ was found and the structural refinement using the XRD data revealed a layered Au···Au network with

Table 3. Selected bond lengths [Å] and angles [°] for powder structures **2**–**5**.

Pr—C(4/9)≡C(5/10)—Cu				Ph—C(7/17)≡C(8/18)—M (M = Cu, Ag, Au)			
2		**3**		**4**		**5**	
Cu1–Cu1	2.44(3)	Cu1–Cu2	2.49(4)	Ag1–Ag2	3.11(1)	Au1–Au1	3.25(1)
Cu1–Cu2	2.61(2)	Cu1–Cu2	2.51(2)	Ag1–Ag2	3.15(1)	Au2–Au2	2.98(1)
		Cu1–Cu2	2.83(2)	Ag1–Ag2	3.13(1)	Au1–Au2	3.175(8)
						Au1–Au2	3.265(8)
Cu1–C5	2.23(2)	Cu1–C8	1.95(1)	Ag1–C8	2.12(1)	Au1–C8	2.151(7)
Cu1–C5	2.05(2)	Cu2–C8	1.94(1)	Ag1–C7	2.71(1)	Au1–C8	2.093(6)
Cu2–C9	2.64(1)	Cu1–C17	2.63(1)	Ag1–C18	2.32(1)	Au1–C18	2.256(7)
Cu2–C5	2.05(2)	Cu1–C18	1.95(1)	Ag2–C8	2.15(2)	Au2–C17	2.415(8)
Cu2–C4	2.48(1)	Cu2–C18	1.93(1)	Ag2–C18	2.12(1)	Au2–C18	2.060(8)
Cu2–C10	2.23(1)	Cu2–C7	2.61(1)			Au2–C18	2.239(9)
Cu2–C10	1.96(1)						
C4–C5	1.25(3)	C7–C8	1.20(4)	C7–C8	1.19(5)	C7–C8	1.182(4)
C9–C10	1.24(6)	C17–C18	1.20(4)	C17–C18	1.19(5)	C17–C18	1.250(5)
Cu1-C5-Cu1	79.2(8)	Cu1-C8-Cu2	93.0(7)	Ag1-C8-Ag2	94.3(4)	Au1-C8-Au2	99.8(3)
Cu2-C10-Cu2	123.7(7)	Cu1-C18-Cu2	80.3(8)	Ag1-C18-Ag2	89.0(4)	Au2-C18-Au2	87.5(5)
Cu1-C5-C4	90.8(5)	Cu1-C8-C7	109.7(7)	Ag1-C8-C7	109.9(7)	Au1-C18-Au2	89.8(5)
	129.8(2)		155.8(6)		157.4(9)		141.7(4)
Cu2-C10-C9	115.0(8)	Cu2-C18-C17	164.5(2)	Ag2-C18-C17	133.5(4)		
	115.7(8)				128.6(5)		

© 2005 Wiley-VCH Verlag GmbH & Co. KGaA, Weinheim

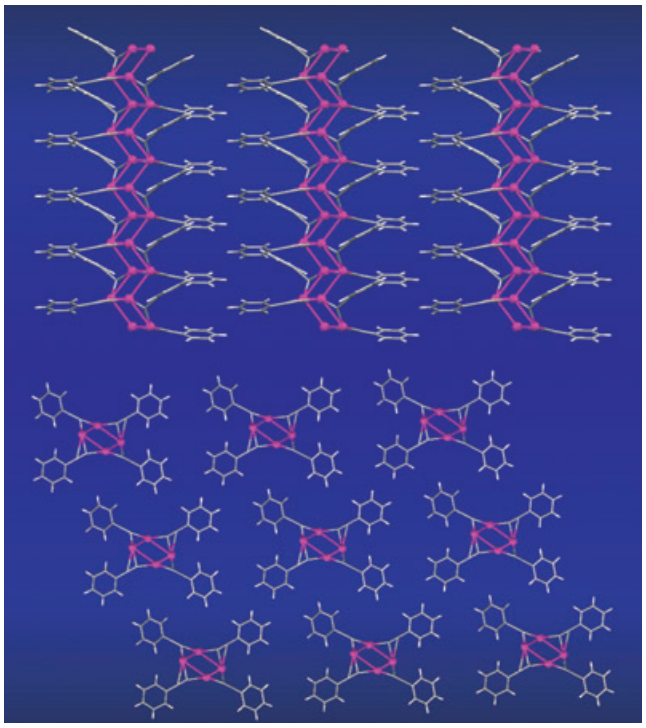

Figure 5. Top: Polymeric chain **4** possessing metal–phenylacetylide connectivity similar to **3**, but with a higher degree of "folding" along the metal chain. Bottom: Perspective view of chain packing of **4** in [010] direction.

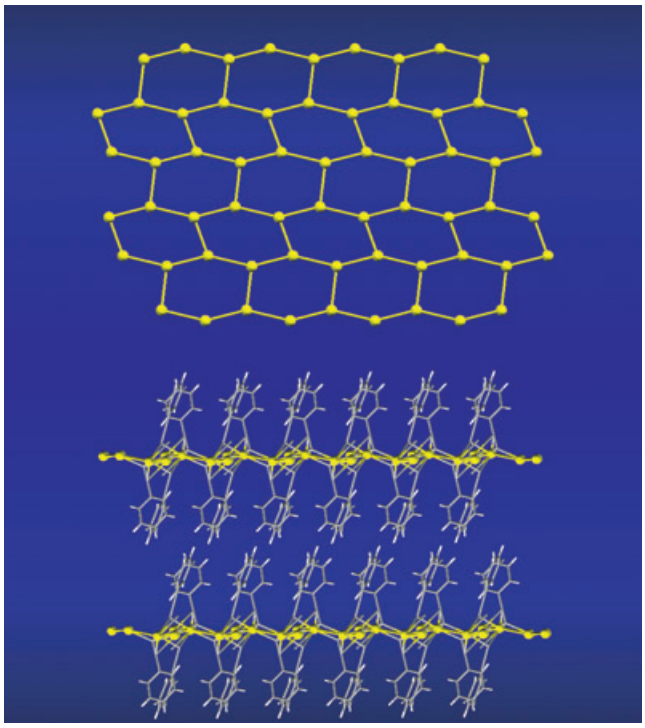

Figure 6. Top: Simplified representation of the distorted two dimensional honeycomb network in **5** with $Au^{I}\cdots Au^{I}$ contacts of 2.98–3.27(1) Å. Bottom: PhC≡C-pillared network in **5** with herringbone-type C–H···π interactions among phenyl rings.

PhC≡C pillars. Figure 6 (top) depicts a schematic representation of the Au–Au honeycomb-like network. In particular the network topology can be viewed as an array of Au···Au distorted hexagons. The Au-Au-Au bond angles associated with Au1 are 97.7, 107.2, and 151.2°; and for Au2 82.9, 123.8, and 151.2°. Comparing with the similar pillared sheet structure **2** [$(n$PrC≡CCu$)_\infty$], half of Cu atoms (Cu1) are slightly displaced by about 0.9 Å from the mean plane generated by the other Cu atoms (Cu2), while in **5** all Au atoms are nearly coplanar to each other. The refined Au···Au contacts are 2.98(1)–3.27(1) Å, which are longer than the metallic radii of Au (2.88 Å)[22b] and comparable to the values (3.083–3.136 Å) of some published polynuclear phenylacetylide gold(I) complexes with phosphine ancillary ligands[5e,g,h] and other gold(I) clusters/polymers.[26a,c,d] Therefore, these gold(I) atoms are weakly interacting[25] within the sheet. Two-dimensional polymeric gold(I) compounds with weak Au···Au interactions (d = 3.104(1) Å) have been shown to display multistate photoluminescence in the solid state.[26b] The theoretical approach to study metallophilic interactions of copper(I), silver(I), and gold(I) developed by Pyykkö et al. and Laguna et al. suggests that metallophilic attraction is indeed present for all coinage metals as a correlation effect and strengthened by relativistic effect for gold.[27]

Unlike the one-dimensional chains in **3** and **4**, two types of coordination modes $\mu,\eta^{1,1}$-C≡C→Au_2 and $\mu_3,\eta^{1,1,2}$-C≡C→Au_3 are noted in **5**. The Au–C distances are 2.060–2.481(8) Å. It is intriguing that the PhC≡C groups coincidentally form pillars on the surface of the Au–Au sheet (Figure 6, bottom) and display a distinctive herringbone-like packing among themselves. Weak hydrogen bonding interactions[28] C–H···π ($d_{C15-H15\cdots C5}$ = 2.63 Å and $d_{C6-H6\cdots C11}$ = 2.75 Å) are observed, while intermolecular phenyl C–H···H–C separations between adjacent sheet polymers are 1.81–2.39 Å. These distances are consistent with optimal hydrophobic interactions among the aromatic rings.

Solid-state photoluminescence: Solid-state emission spectra of **1**–**5** recorded at 298 K and 77 K are depicted in the Figure S6 in the Supporting Information. Excitation of solid **1** at 350 nm gave a red emission with λ_{max} at 720 nm at 298 K. At 77 K, this band is resolved into three peak maxima at 620, 700, and 825 nm. The reason for this is unclear, and probably structural distortion of the molecular cluster or phase transition has occurred. When the same excitation energy was used for solid **2**, the emission spectra recorded at 298 K and 77 K display a similar broad orange emission near 588 nm. In contrast, the room temperature emission spectrum of **3** shows peak maxima at 515, 575, and 618 nm. The emission band at 515 nm is assigned to a metal-perturbed ligand-centered π–π* (acetylide) emission. In addition, another distinctive band of higher energy at 410 nm also merges and may be ascribed to intraligand π–π* emission of phenylacetylide. At 77 K, this high-energy band disappears and λ_{max} of the low-energy emission band is red-shifted to 580 nm. The silver congener **4** shows a yellow-green broad

 © 2005 Wiley-VCH Verlag GmbH & Co. KGaA, Weinheim

emission near 450–700 nm at room temperature. No evident change on the emission spectrum was detected when the solid was cooled to 77 K. In contrast, the emission spectrum of **5** at 298 K displays complex features with several peak maxima at 413, 468, 550, and 592 nm as well as peak shoulders at 621, 636, 653, 670, and 694 nm. In the literature, the emission of gold(I) phenylacetylide complexes in the 500–700 nm region have been attributed to arise from intraligand $^3(\pi\pi^*)$ transition, modified by weak $Au^I\cdots Au^I$ interactions. The photophysics and photochemistry of luminescent polynuclear gold(I) clusters have been extensively investigated in the past decades.[2]

FT-IR spectroscopy: FT-IR spectra of **1**–**5** (Figure S7 in the Supporting Information) show that ν(C≡C) stretching frequencies of the coordinated RC≡C$^-$ ligands are lower than those values found for the free ligands (ν(*t*BuC≡CH) = 2104, ν(*n*PrC≡CH) = 2118, and ν(PhC≡CH) = 2114, 1954, 1888 cm^{-1}). Cluster **1** shows an extremely weak band at 2025–1975 cm^{-1}. This value is slightly lower than that for [(*t*BuC≡CCu)(PPh$_3$)] (2055 cm^{-1})[29a] and resembles that found for the [(*t*BuC≡CCu)$_4$L$_2$] cluster (2001–1976 cm^{-1}; L = 3,3,6,6-tetramethyl-1-thia-4-cycloheptyne).[29b] Two characteristic bands at 1939 and 1900 cm^{-1} in **2** are tentatively assigned to $\mu,\eta^{1,1}$-C≡C and $\mu_3,\eta^{1,1,2}$-C≡C bridging modes, respectively. Indeed, they are comparable to that found for the [(*n*BuC≡C)$_8$Cu$_{18}$(hfac)$_{10}$] disc-shaped cluster (1922 cm^{-1}; hfac = hexafluoroacetylacetonate) reported by Higgs.[30] For the two isostructural chains in **3** and **4**, the bands at 1928 and 1875 cm^{-1} in **3** and 1948 and 1890 cm^{-1} in **4** are attributed to the $\mu,\eta^{1,2}$-C≡C bridging modes. Previous infrared and Raman spectroscopic studies also did not support the presence of two chemically different types of C≡C bonds in the solid-state structure of [{PhC≡CCu}$_\infty$] and [{PhC≡CAg}$_\infty$].[31a,b] The higher energy band at 2052 cm^{-1} in **4** is ascribed to asymmetric C≡C stretching due to weak silver–acetylide interactions.[31c] All these observed frequencies are comparable with related literature values: 1917 cm^{-1} in [(PhC≡CCu)$_4$(Ph$_2$PCH$_2$(CH$_2$OCH$_2$)$_2$CH$_2$PPh$_2$)$_2$],[5i] 2044 cm^{-1} in [(PhC≡CAg)$_4$(PPh$_3$)$_4$],[32b] and 2076 cm^{-1} in [(PhC≡CAg)$_4$(PCy$_3$)$_2$].[5k] Moreover, considering the similar ν(C≡C) bands at 1964, 1983 and 2002 cm^{-1} for the bridging modes in [{(*t*BuC≡CAu)$_6$}$_2$][7] complex, polymer sheet **5** also possesses two similar broad absorption bands at 2019 and 1985 cm^{-1} that are assigned to the doubly and triply bridging modes of the complex. Nevertheless, these values are somewhat lower than those found in the [PhC≡CAu(PCy$_3$)] monomer[5j] (~2113 cm^{-1}) and the [(PhC≡CAu)$_2$(μ-dppe)] dimer[5e] (~2098 cm^{-1}) in which only the terminal σ-bound PhC≡C→Au mode is involved.

TGA studies: The results of the TGA measurements are depicted in Figure S8 in the Supporting Information. From the curves, the residues from compounds **1**–**3** (43% for **1**, 52% for **2** and 49% for **3**) are mainly carbonaceous copper(I) oxide, characterized by energy dispersive analysis of X-ray (EDAX) and powder X-ray diffraction. The pyrolyzed products of **4** and **5** were different from that of Cu^I compounds as only metallic Ag and Au were left. Compounds **1**, **2**, and **5** decomposed at lower onset temperatures (98 °C for **1**, 125 °C for **2**, and 135 °C for **5**) than those for **3** (160 °C) and **4** (185 °C). The molecular cluster **1** exhibits the lowest thermal stability. The polymer sheet **2** is less stable than the chain polymers **3** and **4**, probably due to weaker binding forces associated with the zig-zag Cu$_4$ subunits and the propyl ligands. The color of solid **3** quickly darkened as it was heated at 125 °C, implying that some reaction might have taken place. To examine the possible structural change at elevated temperature, X-ray diffraction data of various annealed solids **3** in 25–650 °C were collected, from which a phase transition between 120–150 °C was found. At 150 °C, the original polymeric structure was completely lost and the formed amorphous material gradually re-crystallized into copper(I) oxide at 650 °C (Figure S9 in the Supporting Information). The reason for poor thermal stability of **5** is unclear and we suggested that a reducing atmosphere during thermal decomposition of these carbon-rich materials has facilitated the formation of those metallic products for **4** and **5**.

Discussion

In this study, the success of using this approach to solve the structures of [(RC≡CM)$_\infty$] is attributed to the following factors: 1) the well-defined and rigid geometry of RC≡C ligand, 2) the availability of metal–carbon bond lengths and known coordination modes of RC≡C→M obtained from previous studies, and 3) the small volume and simplicity of the unit cells. The first factor reduces the numbers of structural variables such as torsion angles of the input model and time spent for locating the chemically sensible structure solution. The second facilitates the evaluation of chemically sensible trial structures generated from the simulated annealing calculations. Finally the last factor implies that fewer symmetry constraints or restrictions in a small lattice space are needed for structure solution searching. The determined structures of complexes **1**–**5** reaffirm that RC≡C ligands are versatile building units and that weak metal–metal interactions are responsible for the formation of polymeric metal–acetylide aggregates. The crystal structure of [*t*BuC≡CCu] cluster systems obtained is strongly dependent upon the crystallization conditions. In contrast to the synthesis of **1** described in this work, the reaction of CuBr·(CH$_3$)$_2$S with *t*BuC≡CLi in diethyl ether produces another oligomer [(*t*BuC≡CCu)$_{24}$].[6] Also in this work, a small amount of yellow plate crystals of [(*t*BuC≡CCu)$_{24}$] in addition to **1** was found if a trace amount of CH$_2$Cl$_2$ or CHCl$_3$ was added into the benzene mother liquid. In addition, Bruce and co-workers reported the rational syntheses of various [*t*BuC≡CM] coordination compounds (M = Cu^I and Ag^I), by using [MCl(PPh$_3$)$_3$] and sodium metal in methanol; however, their crystal structures have not yet been described.[29a] To our knowledge, no polymeric or extended architecture of

© 2005 Wiley-VCH Verlag GmbH & Co. KGaA, Weinheim

$[(t\text{BuC}{\equiv}\text{CM})_\infty]$ has been reported, except for the cationic polymer $[(t\text{BuC}{\equiv}\text{C})_2\text{Ag}_3]^+$, in which the non-coordinating BF_4 anions reside in the channels of the polymer lattice.[33]

Changing the alkyl group from *t*Bu to *n*Pr results in a two-dimensional polymeric sheet formation (See Figure 3 for structure of **2**). The less bulky propyl (butyl) hydrocarbon chains are likely to encapsulate the metal ions to form cluster molecules such as those found in the $[(n\text{BuC}{\equiv}\text{C})_8\text{Cu}_{18}(\text{hfac})_{10}]$ and $[(n\text{PrC}{\equiv}\text{C})_{15}\text{Cu}_{26}(\text{hfac})_{11}]$ (hfac = hexafluoroacetylacetonate) "disc-shaped" clusters reported by Higgs and Tasker.[30,34] In the absence of a coordinated hfac ligand, the propyl substituents form pillars capping the top and bottom of the polymer sheet.

Unlike the alkylacetylides, the formation of isostructural polymer chains **3** and **4** hinges on the role of the phenyl rings in tailoring the crystal structures. The electronic influence and steric demand of phenyl substitutent offers a subtle structural optimization among the metal ions and arylacetylide building units. The less electron-donating phenyl substitutents may not favor high coordination to Cu atoms, unlike the *tert*-butyl substituent in cluster **1**, which displays multidentate μ_3- and μ_4-bridging modes. On the other hand, the planarity of phenyl ring offers a unique molecular handle to induce supramolecular stacking of phenyl groups.

Though the propensity of d^{10} monovalent metals to form oligomeric metal–metal aggregates is anticipated, the formation of extended ladderlike metal aggregates such as those in **3** and **4** is unprecedented. In the literature, a variety of discrete molecular compounds containing $[(\text{PhC}{\equiv}\text{CCu})_n]$ units such as the Cu_2 dimer unit in $[(\text{PhC}{\equiv}\text{CCu})_2(\text{Ph}_2\text{PMe})_4]$,[35] triangular Cu_3 in $[(\text{PhC}{\equiv}\text{C})_n\text{Cu}_3(\mu\text{-dppm})_3][\text{BF}_4]_m$ ($n=1$, $m=2$;[36a] $n=2$, $m=1$[36b]) and $[(\text{PhC}{\equiv}\text{C})_n\text{Cu}_3(\mu\text{-dppm})_3(\mu^3\text{-Cl})][\text{BF}_4]$,[36c] the discrete zig-zag Cu_4 unit in $[(\text{PhC}{\equiv}\text{CCu})_4(\text{PMe}_3)_4]$[37] and $[(\text{PhC}{\equiv}\text{CCu})_4(\text{Ph}_2\text{P-R-PPh}_2)_2]$ complexes (R = $-\text{CH}_2(\text{CH}_2\text{OCH}_2)_2\text{CH}_2$- linker),[5i] as well as the unusual Cu_4 cubanoid unit in $[(\text{PhC}{\equiv}\text{CCu})_4\text{L}_4]$ (L = PPh_3,[38a] PPh_2py = (2-(diphenylphosphine)pyridine,[38b] $\text{P}(p\text{-F-C}_6\text{H}_4)_3$[39] and $\text{P}(p\text{-tolyl})_3$[39]) have been found. All these complexes have low nuclearity and are encapsulated by the bulky phosphine and phenylacetylide ligands. Unlike the PhC≡CCu system, structural investigation on the related PhC≡CAg system remains sparse. A triangular isosceles Ag_3 unit in the $[(\text{PhC}{\equiv}\text{C})_2\text{Ag}_3(\text{dppm})_3]^+$ complex[32a] along with the rhombus-like Ag_4 unit and the square Ag_4 aggregate units in $[(\text{PhC}{\equiv}\text{CAg})_4(\text{PPh}_3)_4]$[32b] and $[(\text{PhC}{\equiv}\text{CAg})_4(\text{PCy}_3)_4]$,[5k] respectively, have previously been reported. In these complexes, Ag···Ag contacts (2.866–3.084 Å) dominate throughout these complexes. Moreover, it is interesting to compare the structures of $[(\text{PhC}{\equiv}\text{CCu})_4(\text{PMe}_3)_4]$ and $[\{(\text{PhC}{\equiv}\text{CAg})(\text{PMe}_3)\}_\infty]$. The former is a molecular complex with a zig-zag Cu_4 unit, while the later forms an extended one-dimensional Ag_∞ chain. The preference of forming an extended structure might be favorable for $[(\text{PhC}{\equiv}\text{CAg})_\infty]$ due to the slightly larger Ag^I ion relative to Cu^I, though the difference in covalent radii of the two metal (1.52 Å for Cu and 1.59 Å for Ag) ions is small.

For the Au^I ion, which has a smaller covalent radius than Cu^I and Ag^I, in the absence of auxiliary ligands, the formed two-dimensional honeycomb Au···Au network polymer in **5** reflects the importance of the phenyl substitutent in directing the final pillared sheet structure of the gold–acetylide complex. The present study complements the earlier work by Mingos et al.[7] on the $[\{(t\text{BuC}{\equiv}\text{CAu})_6\}_2]$ catenane cluster and studies with auxillary phosphine ligands on the PhC≡CAu complexes.[5e,g,h] In **5**, the weak Au···Au interaction and the herringbone-like arrangement of phenyl rings may favor an unrestricted Au···Au network extension along the *ab* direction. The Cambridge Structural Database (CSD) survey on gold(I) compounds reveals that the extended chains[40] and sheet[2b,5h,41] structures are known. However, our present two-dimensional honeycomb network topology in **5** with significant Au···Au interactions is relatively uncommon and contrast to some polymeric examples of $[\{(\text{CN})\text{Au}(\text{CNMe})\}_\infty]$,[41a] $[\{(\text{PhC}{\equiv}\text{C})\text{Au}(2,6\text{-}(\text{Ph}_2\text{P})\text{py})\}_\infty]$,[5h] $[\{(\text{PhC}{\equiv}\text{C})\text{Au}(\text{CNC}_6\text{H}_3\text{Me}_2\text{–}2,6)\}_\infty]$[2b] and $[(\text{tpa})_2\text{Au}][\text{Au}(\text{CN})_2]$ (tpa = 1,3,5-triaza-7-phosphaadamantane)[40g] structures, which show linear arrays of weakly interacting Au^I atoms.

Conclusion

In this work, the structure determination of several [RC≡CM] solids from X-ray powder diffraction data was pursued to unveil the structural complexity of these oligmeric and polymeric species, for which the preparation of sufficiently large crystals for single-crystal diffraction measurements is difficult. Various structures such as discrete molecular clusters, one-dimensional chains, and two-dimensional sheets were formed and these structures are affected by a subtle interplay of 1) electronic and steric features of the RC≡C ligands, 2) metal–metal interactions, and 3) the supramolecular assembly associated with those alkyl/aryl RC≡C ligands. Besides the novelty of these structures, the polymeric nature of the $[(\text{RC}{\equiv}\text{CM})_\infty]$ solid allows extensive d-orbital overlapping for these d^{10} metal ions. In the context of transport properties that had been previously studied by means of theoretical calculations,[42] the electrical conductivity of these one-dimensional polymers might be potentially modified so that the band gaps of these solids can be readily perturbed by adding trace amount of iodine as a dopant.[43] Finally, the complicated solid-state effect on material properties of these polymeric materials demonstrates the importance and necessity of previous studies on related [RC≡CM] molecular analogues.[2b,c,k,5e,5g,5i,5k,30,32–39] Further investigations for other archetypal of this class of compounds are in progress.

Acknowledgement

S.S.Y.C. acknowledges financial support from The University of Hong Kong for the award of a postdoctoral fellowship through the Area of Excellence Scheme (Project No. AoE/P-10/010) and the Research Grants

 © 2005 Wiley-VCH Verlag GmbH & Co. KGaA, Weinheim

Council (RGC) of Hong Kong Special Administration Region (HKSAR) China (Project No. HKU 7039/03P). The author thanks Prof. R. B. Von Dreele and other experts from the public Rietveld mailing list for their fruitful discussion and technical advice in the powder structure determination. Prof. Ian D. Williams and Dr. Hermans H.-Y. Sung of The Hong Kong University of Science and Technology are gratefully acknowledged for their generous help in the single-crystal X-ray data collection.

[1] a) R. Nast, *Coord. Chem. Rev.* **1982**, 47, 89–124; b) B. J. Hathaway, R. J. Lancashire, R. J. Puddephatt, in *Comprehensive Coordination Chemistry*, *Vol. 5* (Eds.: J. A. McCleverty, T. J. Meyer), Elsevier Pergamon, Amsterdam, **1987**, pp. 533–923; c) M. I. Bruce, *Chem. Rev.* **1991**, *91*, 197–257; d) H. Lang, *Angew. Chem.* **1994**, *106*, 569–572; *Angew. Chem. Int. Ed. Engl.* **1994**, *33*, 547–550; e) S. Lotz, P. H. Van Rooyen, R. Meyer, *Adv. Organomet. Chem.* **1995**, 37, 219–320; f) H. Lang, K. Kohler, S. Blau, *Coord. Chem. Rev.* **1995**, 143, 113–168; g) M. D. Janssen, K. Köhler, M. Herres, A. Dedieu, W. J. J. Smeets, A. L. Spek, D. M. Grove, H. Lang, G. van Koten, *J. Am. Chem. Soc.* **1996**, *118*, 4817–4829; h) O. M. Abu-Salah, *J. Organomet. Chem.* **1998**, *565*, 211–216; i) M. A. MacDonald, R. J. Puddephatt, G. P. A. Yap, *Organometallics* **2000**, *19*, 2194–2199; j) H. Lang, D. S. A. George, G. Rheinwald, *Coord. Chem. Rev.* **2000**, 206. 101–197; k) D. Rais, D. M. P. Mingos, R. Vilar, A. J. P. White, D. J. Williams, *Organometallics* **2000**, *19*, 5209–5217; l) D. M. P. Mingos, R. Vilar, D. Rais, *J. Organomet. Chem.* **2002**, *641*, 126–133.

[2] a) X. Hong, K. K. Cheung, C. X. Guo, C.-M. Che, *J. Chem. Soc. Dalton Trans.* **1994**, 13, 1867–1871; b) H. Xiao, K. K. Cheung, C.-M. Che, *J. Chem. Soc. Dalton Trans.* **1996**, 1, 3699–3703; c) B. C. Tzeng, W. C. Lo, C.-M. Che, S. M. Peng, *Chem. Commun.* **1996**, 181–182; d) M. J. Irwin, J. J. Vittal, R. J. Puddephatt, *Organometallics* **1997**, *16*, 3541–3547; e) V. W.-W. Yam, K. K. W. Lo, W. K. M. Fung, C. R. Wang, *Coord. Chem. Rev.* **1998**, 171, 17–41; f) V. W.-W. Yam, K. K. W. Lo, K. M. C. Wong, *J. Organomet. Chem.* **1999**, *578*, 3–30; g) J. P. H. Charmant, J. Forniés, J. Gómez, E. Lalinde, R. I. Merino, M. T. Moreno, A. G. Orpen, *Organometallics* **1999**, *18*, 3353–3358; h) W. J. Hunks, M. A. MacDonald, M. C. Jennings, R. J. Puddephatt, *Organometallics* **2000**, *19*, 5063–5670; i) C.-M. Che, H. Y. Chao, V. M. Miskowski, Y. Li, K. K. Cheung, *J. Am. Chem. Soc.* **2001**, *123*, 4985–4991; j) W. Lu, H. F. Xiang, N. Zhu, C.-M. Che, *Organometallics* **2002**, *21* 2343–2346; k) W. Lu, N. Zhu, C.-M. Che, *J. Am. Chem. Soc.* **2003**, *125*, 16081–16088; l) W. Lu, N. Zhu, C.-M. Che, *J. Organomet. Chem.* **2003**, *670*, 11–16.

[3] a) D. M. Roundhill, J. P. Fackler, Jr., *Optoelectronic Properties of Inorganic Compounds*, Plenum, New York, **1999**, p. 195; b) Y. G. Ma, C.-M. Che, H. Y. Chao, X. M. Zhou, W. H. Chan, J. C. Shen, *Adv. Mater.* **1999**, *11*, 852–857; c) Y. G. Ma, W. H. Chan, X. M. Zhou, C.-M. Che, *New J. Chem.* **1999**, *23*, 263–265; d) W. Lu, B. X. Mi, M. C. W. Chan, C.-M. Che, N. Zhu, S. T. Lee, *J. Am. Chem. Soc.* **2004**, *126*, 4958–4971.

[4] a) H. S. Nalwa, *Handbook of Photochemistry and Photobiology, Vol. 3*, American Scientific, Stevenson Ranch, CA, **2003**, p. 271; b) V. W.-W. Yam, K. L. Cheung, E. C. C. Cheng, N. Zhu, K. K. Cheung, *Dalton Trans.* **2003**, 1830–1835; c) V. W.-W. Yam, S. K. Yip, L. H. Yuan, K. L. Cheung, N. Zhu, K. K. Cheung, *Organometallics* **2003**, *22*, 2630–2637; d) P. K. M. Siu, S. W. Lai, W. Lu, N. Zhu, C.-M. Che, *Eur. J. Inorg. Chem.* **2003**, 2749–2752.

[5] a) O. M. Abu-Salah, A. R. A. Al-Ohaly, C. B. Knobler, *J. Chem. Soc. Chem. Commun.* **1985**, 1502–1503; b) O. M. Abu-Salah, A. R. A. Al-Ohaly, *J. Chem. Soc. Dalton Trans.* **1988**, 2297–2300; c) O. M. Abu-Salah, A. R. A. Al-Ohaly, Z. F. Mutter, *J. Organomet. Chem.* **1990**, *389*, 427–434; d) P. Espinet, J. Forniés, F. Martinez, M. Tomás, E. Lalinde, M. T. Moreno, A. Ruiz, A. J. Welch, *J. Chem. Soc. Dalton Trans.* **1990**, 791–798; e) D. Li, X. Hong, C.-M. Che, W. C. Lo, S. M. Peng, *J. Chem. Soc. Dalton Trans.* **1993**, 2929–2932; f) M. S. Hussian, O. M. Abu-Salah, *J. Organomet. Chem.* **1993**, *445*, 295–300; g) C.-M. Che, H. K. Yip, W. C. Lo, S. M. Peng, *Polyhedron* **1994**, *13*, 887–890; h) S. J. Shieh, X. Hong, S. M. Peng, C.-M. Che, *J. Chem. Soc. Dalton Trans.* **1994**, 3067–3068; i) W. H. Chan, Z. Z. Zhang, T. C. W. Mak, C.-M. Che, *J. Organomet. Chem.* **1998**, *556*, 169–172; j) H. Y. Chao, W. Lu, Y. Q. Li, M. C. W. Chan, C.-M. Che, K. K. Cheung, N. Y. Zhu, *J. Am. Chem. Soc.* **2002**, *124*, 14696–14706; k) Y. Y. Lin, S. W. Lai, C.-M. Che, K. K. Cheung, Z. Y. Zhou, *Organometallics* **2002**, *21*, 2275–2282.

[6] F. Olbrich, J. Kopf, E. Weiss, *Angew. Chem.* **1993**, *105*, 1136–1138; *Angew. Chem. Int. Ed. Engl.* **1993**, *32*, 1077–1079.

[7] D. M. P. Mingos, J. Yau, S. Menzer, D. J. Williams, *Angew. Chem.* **1995**, *107*, 2045–2047; *Angew. Chem. Int. Ed. Engl.* **1995**, *34*, 1894–1895.

[8] D. Rais, J. Yau, D. M. P. Mingos, R. Vilar, A. J. P. White, D. J. Williams, *Angew. Chem.* **2001**, *113*, 3572–3575; *Angew. Chem. Int. Ed.* **2001**, *40*, 3464–3467.

[9] a) W. H. Zachariasen, *Acta Crystallogr.* **1948**, *1*, 265–268; b) W. H. Zachariasen, F. H. Ellinger, *Acta Crystallogr.* **1963**, *16*, 369–375.

[10] a) D. W. Breck, W. G. Eversole, R. M. Milton, T. B. Reed, T. L. Thomas, *J. Am. Chem. Soc.* **1956**, *78*, 5963–5971; b) G. T. Kokotailo, S. L. Lawton, D. H. Olson, W. M. Meier, *Nature* **1978**, *272*, 437–438.

[11] J. E. Berg, P. E. Werner *Z. Kristallogr.* **1977**, 145, 310–320.

[12] a) A. K. Cheetham, A. P. Wilkinson, *Angew. Chem.* **1992**, *104*, 1594–1608; *Angew. Chem. Int. Ed. Engl.* **1992**, *31*, 1557–1570; b) D. M. Poojary, A. Clearfield, *Acc. Chem. Res.* **1997**, *30*, 414–422; c) N. Masciocchi, A. Sironi, *J. Chem. Soc. Dalton Trans.* **1997**, 4643–4650; d) K. D. M. Harris, M. Tremayne, B. M. Kariuki, *Angew. Chem.* **2001**, *113*, 1674–1700; *Angew. Chem. Int. Ed.* **2001**, *40*, 1626–1651; e) V. V. Chernyshev, *Russ. Chem. Bull.* **2001**, 50, 2273–2292; f) "Structure Determination from Powder Diffraction Data": W. I. F. David, K. Shankland, L. B. McCusker, C. Baerlocher, *IUCr Monographs on Crystallography No. 13*, Oxford Science Publications, Oxford (UK), **2002**.

[13] a) D. Blake, G. Calvin, G. E. Coates, *Proc. Chem. Soc. London* **1959**, 396–397; b) G. E. Coates, C. Parkin, *J. Inorg. Nucl. Chem.* **1961**, 22, 59–67; c) G. E. Coates, C. Parkin, *J. Chem. Soc.* **1962**, 3220–3226; d) M. L. H. Green, *Organometallic Compounds Vol. 2, The Transition Elements*, 3rd ed., Barnes and Nobel. New York, **1968**, p. 271; e) E. J. Corey, D. J. Beames, *J. Am. Chem. Soc.* **1972**, *94*, 7210–7211.

[14] a) SADABS, SMART, SAINT (Version 6.01) **1999**, Bruker AXS, Madsion, Wisconsin (USA); b) G. M. Sheldrick, *Acta Crystallogr. Sect. A* **1990**, *46*, 467–473; c) G. M. Sheldrick, SHELX-97, University of Göttingen, Göttingen (Germany), **1997**.

[15] A. Boultif, D. Louer, *J. Appl. Crystallogr.* **1991**, *24*, 987–993.

[16] G. S. Pawley, *J. Appl. Crystallogr.* **1981**, *14*, 357–361.

[17] H. B. Bürgi, J. D. Dunitz, *Structure Correlation*, *Vol. 2*, VCH, New York (USA), **1994**, pp. 767–848.

[18] a) W. I. F. David, K. Shankland, DASH, Program for Structure Solution from Powder Diffraction Data, Cambridge Crystallographic Data Center, Cambridge **2001**. (license agreement No: D/1023/2002); b) H. M. Rietveld, *J. Appl. Crystallogr.* **1969**, *2*, 65–71; c) A. C. Larson, R. B. Von Dreele, *General Structure Analysis System (GSAS)*, Report LAUR 86–748, Los Alamos National Laboratory, NM **1994**.

[19] A crystal structure visualization software: Mercury 1.2 can be downloaded free of charge from the following URL http://www.ccdc.cam.ac.uk/mercury/.

[20] Crystal data of **1**: triclinic $P\bar{1}$, $a=16.607(1)$, $b=16.893(1)$, $c=25.705(1)$ Å, $\alpha=76.738(1)°$, $\beta=83.820(1)°$, $\gamma=69.050(1)°$, $V=6552.4(5)$ Å^3, $Z=2$, $M_r=2971.5$, $T=233$ K, $\rho_{calcd}=1.506$ g cm^{-3}, $\mu(Mo_{K\alpha})=3.210$ mm^{-1}, $F(000)=3044$, reflections = 30288 [R(int) = 0.0552], data/parameters = 30288/1325, goodness-of-fit on $F^2=1.000$, final R indices for $I>2\sigma(I)$: $R1=0.0644$, $wR2=0.1184$, largest peak/hole = 1.245/−0.993 e Å^{-3}. All non-hydrogen atoms were refined anisotropically, except the following methyl carbon pairs: C3F & C3G, C5E & C5H, C8E & C8H, C11E & C11H, C11D & C11I, C12D & C12I. Due to structural disorder, they were treated with 50:50 split occupancies and each thermal parameter was isotropically refined. The refined occupancy factors of 75% and 25% were determined for Cu18 and its minor component Cu18′ respectively. All methyl hydrogen atoms were constrained in the idealized positions with dis-

© 2005 Wiley-VCH Verlag GmbH & Co. KGaA, Weinheim

placement parameters 1.5 times of those of the attached carbons. One benzene molecule was located per one cluster molecule.

[21] a) D. Fenske, H. Krautscheid, *Angew. Chem.* **1990**, *102*, 1513–1516; *Angew Chem. Int. Ed. Engl.* **1990**, *29*, 1452–1454; b) H. Krautscheid, D. Fenske, G. Baum, M. Semmelmann, *Angew. Chem.* **1993**, *105*, 1364–1367; *Angew Chem. Int. Ed. Engl.* **1993**, *32*, 1303–1305; c) D. Fenske, J. C. Steck, *Angew. Chem.* **1993**, *105*, 254–257; *Angew Chem. Int. Ed. Engl.* **1993**, *32*, 238–242; d) S. Dehnen, D. Fenske, *Angew. Chem.* **1994**, *106*, 2369–2372; *Angew Chem. Int. Ed. Engl.* **1994**, *33*, 2287–2289; e) S. Dehnen, D. Fenske, *Chem. Eur. J.* **1996**, *2*, 1407–1416; f) A. Deveson, S. Dehnen, D. Fenske, *J. Chem. Soc. Dalton Trans.* **1997**, 4491–4498; g) A. Eichhofer, D. Fenske, *J. Chem. Soc. Dalton Trans.* **1998**, 2969–2972; h) M. Bettenhausen, A. Eichhofer, D. Fenske, M. Semmelmann, *Z. Anorg. Allg. Chem.* **1999**, 625, 593–601; i) N. Zhu, D. Fenske, *J. Chem. Soc. Dalton Trans.* **1999**, 1067–1076; j) D. Fenske, N. Zhu, *J. Cluster Sci.* **2000**, *11*, 135–151.

[22] a) J. C. Slater, *J. Chem. Phys.* **1964**, *41*, 3199–3204; b) J. Emsley, *The Elements*, Clarendon, Oxford, UK, **1989**, p. 192.

[23] a) J. M. Zuo, M. Kim, M. O'Keeffe, J. C. H. Spence, *Nature* **1999**, *401*, 49–52; b) C.-M. Che, Z. Mao, V. M. Miskowski, M. C. Tse, C. K. Chan, K. K. Cheung, D. L. Philips, K. H. Leung, *Angew. Chem.* **2000**, *112*, 4250–4254; *Angew. Chem. Int. Ed.* **2000**, *39*, 4084–4088; c) H. L. Hermann, G. Boche, P. Schwerdtfeger, *Chem. Eur. J.* **2001**, *7*, 5333–5342; d) L. Magnko, M. Schweizer, G. Rauhut, M. Schütz, H. Stoll, H. J. Werner, *Phys. Chem. Chem. Phys.* **2002**, *4*, 1006–1013; e) Z. Mao, H. Y. Chao, Z. Hui, C.-M. Che, W. F. Fu, K. K. Cheung, N. Zhu, *Chem. Eur. J.* **2003**, *9*, 2885–2894; f) W. F. Fu, X. Gan, C.-M. Che, Q. Y. Cao, Z. Y. Zhou, N. Zhu, *Chem. Eur. J.* **2004**, *10*, 2228–2236.

[24] a) M. Jansen, *Angew. Chem.* **1987**, *99*, 1136–1149; *Angew. Chem. Int. Ed. Engl.* **1987**, *26*, 1098–1110; b) C.-M. Che, H. K. Yip, D. Li, S. M. Peng, G. H. Lee, Y. M. Wang, S. T. Liu, *J. Chem. Soc. Chem. Commun.* **1991**, 1615–1617; c) K. Singh, J. R. Long, P. Stavropoulos, *J. Am. Chem. Soc.* **1997**, *119*, 2942–2943; d) A. J. Blake, N. R. Champness, A. N. Khlobystov, D. A. Lemenovskii, W. S. Li, M. Schröder, *Chem. Commun.* **1997**, 1339–1340; e) M. A. Omary, T. R. Webb, Z. Assefa, G. E. Shankle, H. H. Patterson, *Inorg. Chem.* **1998**, *37*, 1380–1386; f) G. C. Guo, T. C. W. Mak, *Angew. Chem.* **1998**, *110*, 3296–3299; *Angew. Chem. Int. Ed.* **1998**, *37*, 3183–3186; g) G. C. Guo, G. D. Zhou, Q. G. Wang, T. C. W. Mak, *Angew. Chem.* **1998**, *110*, 652–654; *Angew. Chem. Int. Ed. Engl.* **1998**, *37*, 630–632; h) D. Fenske, N. Zhu, T. Langetepe, *Angew. Chem.* **1998**, *110*, 2783–2788; *Angew. Chem. Int. Ed. Engl.* **1998**, *37*, 2639–2644; i) G. C. Guo, G. D. Zhou, T. C. W. Mak, *J. Am. Chem. Soc.* **1999**, *121*, 3136–3141; j) C.-M. Che, M. C. Tse, M. C. W. Chan, K. K. Cheung, D. L. Philips, K. H. Leung, *J. Am. Chem. Soc.* **2000**, *122*, 2464–2468; k) Q. L. Wang, T. C. W. Mak, *J. Am. Chem. Soc.* **2000**, *122* 7608–7609; l) Q. L. Wang, T. C. W. Mak, *J. Am. Chem. Soc.* **2001**, *123*, 1501–1502.

[25] H. Schmidbaur, *Chem. Soc. Rev.* **1995**, *24*, 391–400; *Gold Bull.* **2000**, *33*, 3–10.

[26] a) R. M. Dávila, A. Elduque, T. Grant, R. J. Staples, J. P. Fackler, Jr., *Inorg. Chem.* **1993**, *32*, 1749–1755; b) B. C. Tzeng, K. K. Cheung, C.-M. Che, *Chem. Commun.* **1996**, 1681–1682; c) W. Schneider, A. Bauer, H. Schmidbaur, *Organometallics* **1996**, *15*, 5445–5446; d) A. Burini, J. P. Fackler, Jr., R. Galassi, B. R. Pietroni, R. J. Staples, *Chem. Commun.* **1998**, 95–96.

[27] a) P. Pyykkö, *Chem. Rev.* **1997**, *97*, 597–636; b) P. Pyykkö, F. Mendizabal, *Inorg. Chem.* **1998**, *37*, 3018–3025; c) P. Pyykkö, N. Runeberg, F. Mendizabal, *Chem. Eur. J.* **1997**, *3*, 1451–1457; d) E. J. Fernández, J. M. López-De-Luzuriaga, M. Monge, M. A. Rodríguez, O. Crespo, M. C. Gimeno, A. Laguna, P. G. Jones, *Chem. Eur. J.* **2000**, *6*, 636–644, and references therein.

[28] "The Weak Hydrogen Bond in Structural Chemistry and Biology":G. Desiraju, T. Steiner, *IUCr Monograph on Crystallography, No. 9*, Oxford University Press, New York, **1999**, pp. 155–158.

[29] a) M. I. Burce, M. G. Humphrey, J. G. Matisons, S. K. Roy, A. G. Swincer, *Aust. J. Chem.* **1984**, *37*, 1955–1961; b) F. Olbrich, U. Behrens, E. Weiss, *J. Organomet. Chem.* **1994**, *472*, 365–370.

[30] T. C. Higgs, S. Parsons, A. C. Jones, P. J. Bailey, P. A. Tasker, *J. Chem. Soc. Dalton Trans.* **2002**, 3427–3428.

[31] a) I. A. Garbuzova, V. T. Aleksanyan, L. A. Leites, I. R. Golding, A. M. Sladkov, *J. Organomet. Chem.* **1973**, *54*, 341–344; b) V. T. Aleksanyan, I. A. Garbuzova, I. R. Golding, A. M. Sladkov, *Spectrochim. Acta Part A* **1975**, *31*, 517–524; c) P. W. R. Corfield, H. M. M. Shearer, *Acta Crystallogr.* **1966**, *20*, 502–508.

[32] a) C. F. Wang, S. M. Peng, C. K. Chan, C.-M. Che, *Polyhedron* **1996**, *15*, 1853–1858; b) C. Brasse, P. R. Raithby, M. A. Rennie, C. A. Russell, A. Steiner, D. S. Wright, *Organometallics* **1996**, *15*, 639–644.

[33] K. A. Al-Farhan, M. H. Ja'far, O. M. Abu-Salah, *J. Organomet. Chem.* **1999**, *579*, 59–62.

[34] T. C. Higgs, P. J. Bailey, S. Parsons, P. A. Tasker, *Angew. Chem.* **2002**, *114*, 3164–3167; *Angew. Chem. Int. Ed.* **2002**, *41*, 3038–3041.

[35] V. W.-W. Yam, W. K. Lee, K. K. Cheung, H. K. Lee, W. P. Leung, *J. Chem. Soc. Dalton Trans.* **1996**, 2889–2891.

[36] a) M. P. Gamasa, J. Gimeno, E. Lastra, A. Aguirre, S. García-Granda, *J. Organomet. Chem.* **1989**, *378*, C11–C14; b) J. Diéz, M. P. Gamasa, J. Gimeno, A. Aguirre, S. García-Granda, *Organometallics* **1991**, *10*, 380–382; c) J. Diéz, M. P. Gamasa, J. Gimeno, E. Lastra, A. Aguirre, S. García-Granda, *Organometallics* **1993**, *12*, 2213–2220.

[37] P. W. R. Corfield, H. M. M. Shearer, *Acta Crystallogr.* **1966**, *21*, 957–965.

[38] a) L. Naldini, F. Demartin, M. Manassero, M. Sansoni, G. Rassu, M. A. Zoroddu, *J. Organomet. Chem.* **1985**, *279*, C42-C44; b) M. P. Gamasa, J. Gimeno, E. Lastra, X. Solans, *J. Organomet. Chem.* **1988**, *346*, 277–286.

[39] V. W.-W. Yam, W. K. Lee, K. K. Cheung, *J. Chem. Soc. Dalton Trans.* **1996**, 2335–2339.

[40] a) P. W. R. Corfield, H. M. M. Shearer, *Acta Crystallogr.* **1967**, *23*, 156–162; b) D. Parker, P. S. Roy, G. Ferguson, M. M. Hunt, *Inorg. Chim. Acta* **1989**, 155, 227–230; c) H. Schmidbaur, G. Weidenhiller, O. Steigelmann, G. Müller, *Z. Naturforsch. B* **1990**, *45*, 747–752; d) S. Ahrland, B. Aurivillius, K. Dreisch, B. Norén, *Acta Chem. Scand.* **1992**, *46*, 262–265; e) S. Ahrland, K. Dreisch, B. Norén, A. Oskarsson, *Mater. Chem. Phys.* **1993**, 35, 281–289; f) K. Angermaier, E. Zeller, H. Schmidbaur, *J. Organomet. Chem.* **1994**, *472*, 371–376; g) Z. Assefa, M. A. Omary, B. G. McBurnett, A. A. Mohamed, H. H. Patterson, R. J. Staples, J. P. Fackler, Jr., *Inorg. Chem.* **2002**, *41*, 6274–6280.

[41] a) S. Esperås, *Acta Chem. Scand. Ser. A* **1976**, *30*, 527–530; b) P. G. Jones, *Z. Naturforsch. B* **1982**, *37*, 823–824.

[42] Z. M. Su, R. S. Wang, C.-M. Che, *Mater. Res. Soc. Symp. Proc.* **1999**, 576 389–394.

[43] a) X. Gan, M. Munakata, T. Kuroda-Sowa, M. Maekawa, M. Yamamoto, *Polyhedron* **1995**, *14*, 1647–1651; b) M. Yamamoto, X. Gan, T. Kuroda-Sowa, M. Maekawa, Y. Suenaga, M. Munakata, *Inorg. Chim. Acta* **1997**, 261, 169–174; c) J. Dai, M. Munakata, T. Kuroda-Sowa, Y. Suenaga, L. P. Wu, M. Yamamoto, *Inorg. Chim. Acta* **1997**, 255, 163–166; d) Y. Suenaga, T. Kuroda-Sowa, M. Munakata, M. Maekawa, H. Morimoto, *Acta Crystallogr. Sect. C* **1998**, *54*, 1566–1569; e) T. Okubo, T. Ohrui, M. Kondo, S. Kitagawa, H. Matsuzaka, *Synth. Met.* **1999**, 102, 1464–1465; f) J. C. Zhong, Y. Misaki, M. Munakata, T. Kuroda-Sowa, M. Maekawa, Y. Suenaga, H. Konaka, *Inorg. Chem.* **2001**, *40*, 7096–7098; g) B. J. McCormick, C. Siemer, F. Afroz, J. R. Wasson, D. M. Eichhorn, B. Scott, S. Shah, K. Noffsinger, P. K. Kahol, *Synth. Met.* **2001**, 120, 969–970.

Received: August 27, 2004
Published online: January 24, 2005

 © 2005 Wiley-VCH Verlag GmbH & Co. KGaA, Weinheim